# DETECTION OF AN ACOUSTIC SOURCE INSIDE A PIPE USING OPTIMIZED VIBROACOUSTIC BEAMFORMING

Souha Kassab, Laurent Maxit, Frédéric Michel

25th International Congress on Sound and Vibration
8-12 July 2018 HIROSHIMA CALLING
ICSV25

# DETECTION OF AN ACOUSTIC SOURCE INSIDE A PIPE USING OPTIMIZED VIBROACOUSTIC BEAMFORMING

[1] Souha Kassab[(1,2)], Laurent Maxit[(1)], Frédéric Michel[(2)].

*[(1)]Laboratoire Vibrations acoustique (LVA), Institut National Supérieur des Sciences Appliqués, Lyon, France ;*

*[(2)] CEA, DEN, DTN/STCP/LISM, Cadarache, France;*

*[(3)] PRISME/P12/EDF R&D-EDF/ Chatou, France.*

In an intent to improve the monitoring of steam generators, a technique based on vibration measurements is developed for the detection of a water leak into sodium. Background noise can mask the leak-induced vibrations. In order to increase the signal-to-noise ratio (SNR), a beamforming technique may be considered. In the purpose of studying the feasibility and the efficiency of this technique for the present configuration, experimental investigations have been performed on a mock-up composed by a straight cylindrical pipe coupled to a hydraulic circuit through two flanges. A sound emitter introduced in the pipe simulates the source to detect, whereas a varying flow speed controls the background noise vibrations. Beamforming is applied on the signals measured by an array of accelerometers externally mounted on the pipe. Two different kinds of beamforming are considered: the conventional (Bartlett*)* one and a statistically optimized one based on SNR maximization. After a brief presentation of the mock-up's vibroacoustic characteristics, we study the efficiency of the two beamforming treatments for narrowband and broadband analysis.

Keywords: beamforming, leak detection, pipe, heavy fluid.

## 1. Introduction

This paper describes the study of a non-intrusive vibroacoustic beamforming technique aimed at the detection of sodium-water reactions in the steam generator of a liquid sodium fast reactor (SFR). Vibroacoustic beamforming previously developed within a PhD thesis by J. Moriot is reconsidered [1]. Beamforming over an array of sensors is of main interest due to its ability to increase the signal-to-noise ratio of the chemical reaction acoustic signals, generally masked by the high power plant background noise. Thus, we can provide a quantitative estimation of the SNR increase at the beamforming output relative to the SNR on the reference sensor using the "effective gain". From the detection on a threshold criterion at the output of beamforming (instead of the reference sensor), this gain allows the improvement of the detection rate while limiting the array sensibility to false alarms. Moriot's thesis showed promising results. However, the latter were obtained by the means of academic numerical test models (plate or infinite shell coupled to a heavy fluid) or from experimental data at some harmonic frequencies [2]. To carry out new investigations on a "broad" frequency band, we have taken up the test duct constructed in J. Moriot's thesis. Thus, the source to be detected consists of a hydrophone in transmission mode placed inside the test duct (i.e. cylindrical pipe) which

[1] Emails of Authors to contact :
souha.kassab@insa-lyon.fr; laurent.maxit@insa-lyon.fr.

is itself connected to the hydraulic circuit by two flanges. Disturbance noise is induced by a supposedly turbulent water flow with a given flow-rate. The antenna (or array) whose signals are beamformed is constituted by 25 accelerometers positioned on the vein line.

Figure 1 represents a diagram of the mock-up configuration considered in this study. The purpose of the beamforming is to simultaneously process the sensors' measurements (i.e. spatial filtering) to bring out the source while rejecting the flow-induced vibration noise.

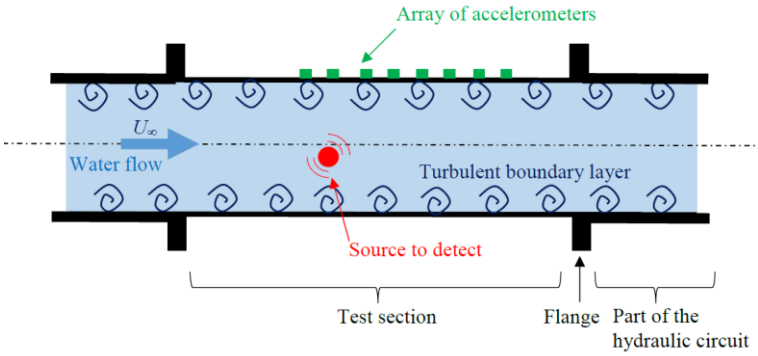


Figure 1.Schematic representation of the configuration considered to study the performance of the formation of vibro-acoustic pathways.

## 2. Classical and MaxSNR beamfomring

We recall that beamforming consists of "spatially" filtering the signals registered by the antenna. If we denote by Γ the cross-spectral matrix of the signals received by the array of sensors and by $F_u$ the steering vector (i.e. spatial filtering vector) which points at the position u of the detection space, then the level $y_u$ at the beamforming output, is given by:

$$y_u = F_u^* \Gamma F_u. \tag{1}$$

Assuming that the signal to be detected and the noise is independent, we can decompose the matrix Γ as such:

$$\Gamma = \Gamma_s + \Gamma_b, \tag{2}$$

where $\Gamma_s$ is the cross-spectral matrix of the signals induced by the source alone and $\Gamma_b$ is the cross-spectral matrix of the signals induced by the noise alone.

Assuming that the noise is homogeneous and spatially incoherent (i.e. $\Gamma_b = \sigma_b I$) with I the identity matrix), it can be shown that the array gain – defined as the ambiguity function maximum value for an incoherent background noise – is maximum when the steering vector is given by:

$$F_u^{class} = \frac{H_u}{\|H_u\|^2}, \tag{3}$$

where $H_u$ is the vector containing the transfer functions between the (assumed) position u of the source and the antenna's accelerometers (i.e. sensors).

This beamforming technique relies on a prior knowledge of the source (through the transfer functions) as well as on the assumption that the noise would appear spatially incoherent. This is what will later be called the "classical" beamforming method.

However, numerical and experimental tests presented in section 4.5 show that the vibration noise recorded by the array's sensors (i.e. accelerometers) exhibits some spatial coherence. Inevitably, this will lead to a deterioration in the performance of classical beamforming compared to what could be assumed for the latter if the vibration noise showed perfect incoherence.

To overcome this obstacle, different variants of beamforming based on prior knowledge of noise have been developed [3]. We can notably cite one that seeks to maximize the signal-to-noise ratio at

the beamforming output, knowing the cross-spectral noise matrix. The steering vector is then defined as follows:

$$F_u^{opt} = \arg\left[\max\left(\frac{F_u^* \Gamma_s F_u}{F_u^* \Gamma_b F_u}\right)\right]. \quad (4)$$

Algebraic considerations[4] show that the solution to eq. 4 can be written by an eigenvector associated with the greatest eigenvalue of the matrix:

$$\Gamma_b^{-1} \Gamma_s F_u^{opt} = \lambda_{max} F_u^{opt}. \quad (5)$$

The steering vectors thus defined allow the maximization of the signal-to-noise ratio at the output of beamforming. The technique nevertheless presents the disadvantage of requiring a generalized eigenvalues problem resolution, which can induce numerical instabilities. It also requires knowledge of the noise cross-spectral matrix. In practice, this can be estimated from *in-situ* measurements with the sensor antenna when no source is assumed present in the pipe. An average over a set of measured signals samples can be performed regularly to take into account the evolution of the cross-spectral noise matrix in the system as a function of time.

## 3. Presentation of the experimental mock-up

The test duct presented in Figure 2 aims to study the performance of the beamforming technique for detecting an acoustic source in a heavy fluid, using vibratory measurements on the ferrule. In this experiment, the steam generator shell is represented by a cylindrical pipe made of stainless steel. For the ease of implementation and safety reasons, the fluid used inside the pipe water (rather than sodium) at room temperature, and at a pressure of about 4 bars. The duct is connected to the hydraulic circuit by two rigid clamps. Special attention has been paid by the technical team of Le Centre Technique du Creusot (Framatome enterprise) where the mock-up is established to decouple the vein from external mechanical stresses (suspended slabs, fixing of the pipe with rubber seals) and acoustic (decoupling balloons).

To simulate a monopole source (theoretically equivalent to a water-sodium reaction), we use a *B&K 8103* hydrophone in transmission mode to generate a harmonic sound signal at different axial positions within the pipe, using different taps. A mechanical device (see Figure 3) dedicated to the insertion of the hydrophone inside the pipe is also developed. This device allows us to control the hydrophone's radial position. The selected hydrophone allows to have a source of relatively small size. On the other hand, because of its size, this device has the drawback of accounting for an acoustic source that's not very effective in the frequency band of interest (i.e.$0.5\ \text{kHz} - 5\text{kHz}$). It follows that the signal-to-noise ratio is too low to have truly exploitable measurements below 2 kHz.

The pipe vibrations are measured by a *KISTLER 8704B50* accelerometer array. beamforming is then applied to the array signals to detect the hydrophone. Primary and secondary pumps are monitored by a dedicated software that makes it possible to obtain different water flows in the pipe (thus different signal-to-noise ratio), for different positions of the source as well as for different array configuration. Nevertheless, we will present the following results for a unique dataset:

—The flow rate is: $Q_w = 140\ l.s^{-1}$;

—The source is positioned in $(\mathrm{x_s}, \mathrm{r_s}, \theta_\mathrm{s}) = (0.56\mathrm{m}, 0.05\mathrm{m}, 0°)$ in the cylindrical coordinate system shown in Figure 3.

—The antenna is linear: accelerometers have been positioned according to the plane $\theta = -90°$ of the pipe. The spacing between the sensors is $\Delta\mathrm{x} = 4\ \text{centimeters}$. The first sensor being positioned at 12 centimeters from the upstream flange of the flow ($x_1 = -0.12m$).

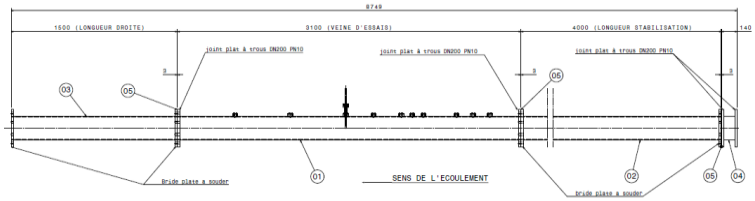


Figure 2. View of the test duct connected to the hydraulic circuit (downstream stabilization section and upstream discharge section).

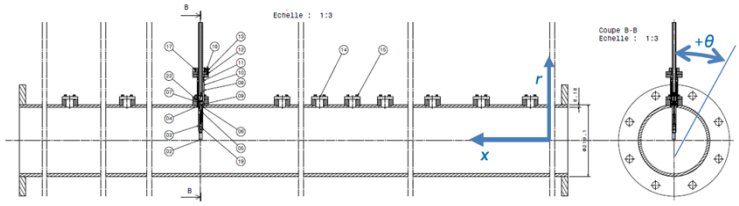


Figure 3. View of the model with the various holes to insert the hydrophone. Cylindrical coordinates marked in blue.

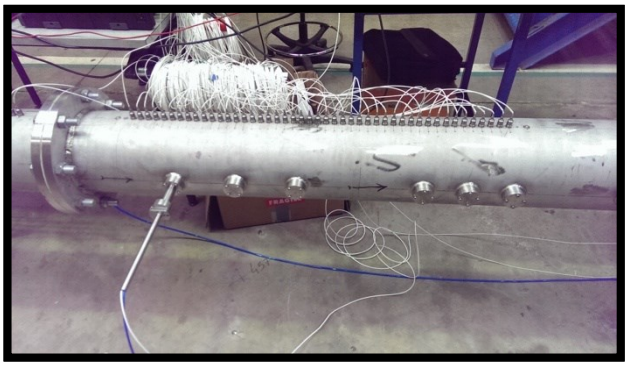

Figure 4. Picture of the instrumented conduct

## 4. Study of the pipe vibroacoustic behaviour

Figure 5.a shows the vibratory field measured for a radial mechanical excitation (i.e. impact hammer) applied in x = 0.105 m, that is to say near a flange. The levels were reduced to a unit radial force (i.e. 1 N). It is preferable to display the results in terms of radial displacements rather than in terms of radial accelerations since the displacements present the same dynamics throughout the frequency range considered. It can be pointed out that the sensor in x = 0.6 m seems to have a malfunction. These results were compared to a numerical model of a thin shell coupled to two axi-symmetric stiffeners presented in [5] (results not shown). Good agreement between numerical and experimental results were observed. The different results analysis shows that high vibration levels observed at 372 Hz and 1072 Hz (see Figure 5.a) are due to the circumferential modes n = 2 and n = 3 cut-on at these frequencies, respectively [6], [7]. Moreover, the resonances observed for frequencies higher than these two values correspond to pseudo-axial modes. These are induced by the presence of connecting flanges which appear highly rigid and causing the fluid-shell coupled waves to reflect upon them.

At Figure 5.b, we are rather concerned by the flow-induced signal's coherence in absence of an acoustic source, which can influence the performance of the beamforming. In the presence of the fluid at rest (only booster pump in operation), the signals between the different accelerometers seem rather incoherent. However, for a flow rate of $140\ \mathrm{l.s^{-s}}$, it can be seen that the signals are highly coherent for frequencies corresponding to resonant frequencies of the system (by comparing Fig.5.a and 5.b.) This occurs well below1 kHz. Above 1kHz, it seems less obvious. However, it must be recalled that an excitation applied on the vein near a flange will not excite all the axial modes of the shell. An

excitation further away from the flanges would have made it possible to bring out axial modes relating to the circumferential orders n = 0 and n = 1. Although the pressure fluctuations induced by the turbulent flow have very weak correlations at the scale of the separation between the sensors [i.e. 4 cm], the vibration field induced by them has a strong spatial coherence at the resonance frequencies of the system. This could be confirmed by numerical testing (see [8]).

As we will see, this strong coherence of the signals over the antenna sensors can be very damaging for the classical beamforming.

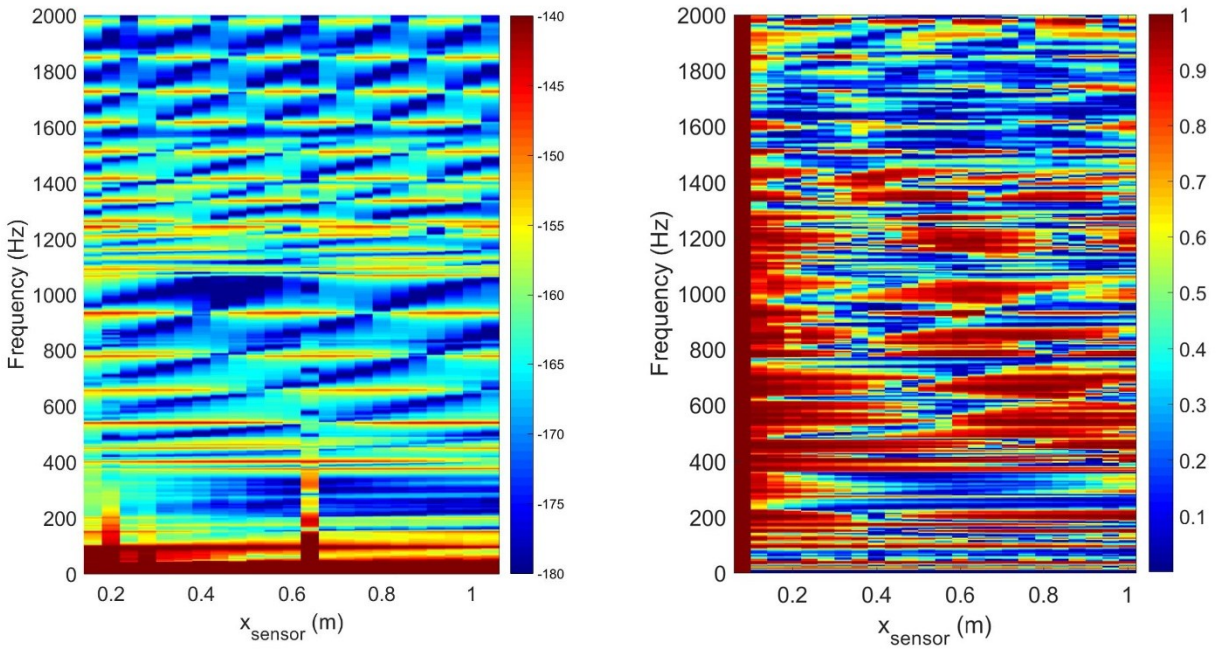


(a) (b)

Figure 5. (a) Levels of displacement measured by the antenna sensors for mechanical excitation in x = 0.105 m. Experimental results; (b) Standardized cross-spectral matrices of accelerations between sensor # 1 and sensor i for a flow rate $Q_w = 140\,\mathrm{l.s^{-1}}$.

## 5. Performance analysis of beamforming

### 5.1 Reference sensor and effective antenna gain

In order to compare the performance of beamforming techniques, it is necessary to have a reference indicator of the pre-filtering state. For this, we will define the SNR of a sensor as the ratio of the autospectrum of the source-to-detect induced signals in absence of any perturbing noise, to that induced by the noise alone, in absence of all source. This means the SNR might vary from one sensor to another. The one with the highest signal-to-noise ratio (SNR) at the frequency considered will define the "reference" sensor.

In Fig. 5, we present the level of the SNR on the reference sensor and its number according to the frequency. We notice that the levels on all the sensors increase with the frequency. We can observe a general tendency of the SNR increase with frequency, which is, on the one hand, due to an increase in the radiation of the source and, on the other hand, to a decrease in noise induced by the flow. In addition, the reference sensor changes from one frequency to another. This definition of the SNR reference value is only optimal for detection from a single sensor for narrow band analysis. Nevertheless, in practice, it will not seem very relevant for the detection of broadband sources. For broadband analysis, the SNR of a sensor is defined as the ratio of the source-induced signal level induce alone in the band of interest, to the level of noise alone in the same band. The reference sensor remains the one with the strongest SNR for the broadband in question. The reference SNR and

reference sensor index for 500 Hz bands are shown in Fig. 6.b. Overall, the reference SNR per band is lower than that presented for narrow bands. The reason of this resides in the fact that reference sensor does not change for the frequencies contained in the same frequency band.

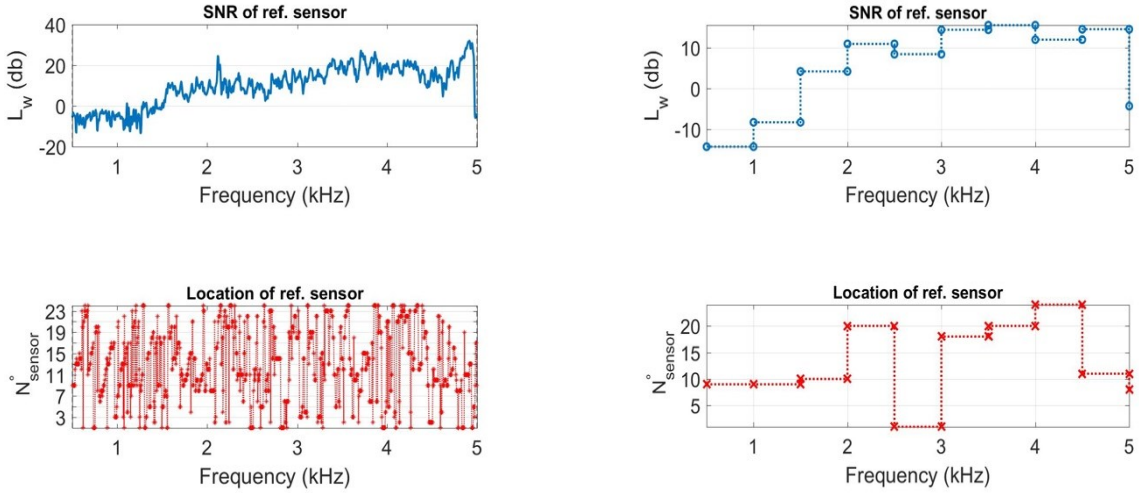


(a) (b)

Figure 6. Signal to noise ratio and reference sensor number. (a) Narrow-band analysis; (b) Broadband analysis

## 5.2 Beamforming results

Subsequently, we present the results of classical beamforming output and MaxSNR beamforming with steering vectors defined from equations (3) and (5), respectively. The transfer functions $H_u$ between the sensors and the source involved in the definition of these steering vectors have been obtained experimentally from acquisitions in the presence of a source without water flow. We recall that, given the size of the hydrophone, the coherence between the signal of the source and the signals received by the antenna appears rather weak for the frequencies between 500 Hz and 2 kHz. We will therefore consider the results below 2 kHz with caution. For optimized beamforming, we consider the cross-spectral matrix of signals between the sensors in the absence of the source for the flow rate considered ($140\ \mathrm{l.s^{-1}}$).

### *5.2.1 Narrow and broadband investigation*

Beamforming is applied for the hydrophone signal without water flow in the mock-up, as well as for the non-signaling flow noise signal. We illustrate in Fig. 7 the output levels of classical and optimized beamforming for the case where there is only the source to detect (i.e. source with a zero flow) or where there is only noise (i.e. no source with a flow rate of 140 l / s). It can be seen that the differences between the signal output levels of the signal and the noise appear generally greater for optimized beamforming than for the conventional one. These differences are mainly due to the fact that the output level of beamforming for the noise is lowered by the optimized treatment with respect to the conventional treatment. Optimized processing seems better at rejecting noise than conventional processing (which results from its definition).

From the previous results, we can calculate the SNR at the output of beamforming. By substracting with the SNR on the reference sensor, we obtain the effective antenna gain for the 2 treatments. The results are shown in Fig. 8.

We observe that conventional treatment does not significantly increase the SNR. The effective gain takes null, or even negative values (which accounts for an actual loss in the SNR values with respect to the reference values). This can be attributed to the fact that the vibrating noise induced by a flow at $140\,\mathrm{l.s^{-1}}$ is strongly spatially correlated as we have seen in Fig. 4.b. For optimized beamforming, an effective gain that ranges between 5 dB and 25 dB is observed. This treatment makes it possible to reject the noise even if it is strongly correlated spatially. Next, we consider the analysis on frequency bands of 500 Hz width. It is recalled that the SNR of the reference sensor was given in Fig. 6.b by integrating on each band the signals in narrow bands obtained at the output of beamforming. Beamforming output levels per band are obtained for the source alone and for the noise alone. We deduce the SNR of the beamforming output and the effective gain for each band. The results are presented in Fig. 8. Overall results observed in thin bands are reproduced. Conventional beamforming gives poor results while the effective gain for optimized beamforming varies between 9 dB and 23 dB, which looks very significant and encouraging. It is slightly higher than that observed in thin bands. This can be attributed to the fact that the SNR on the reference sensor comes across as lower during a frequency broad-band analysis than when a narrow band analysis is performed.

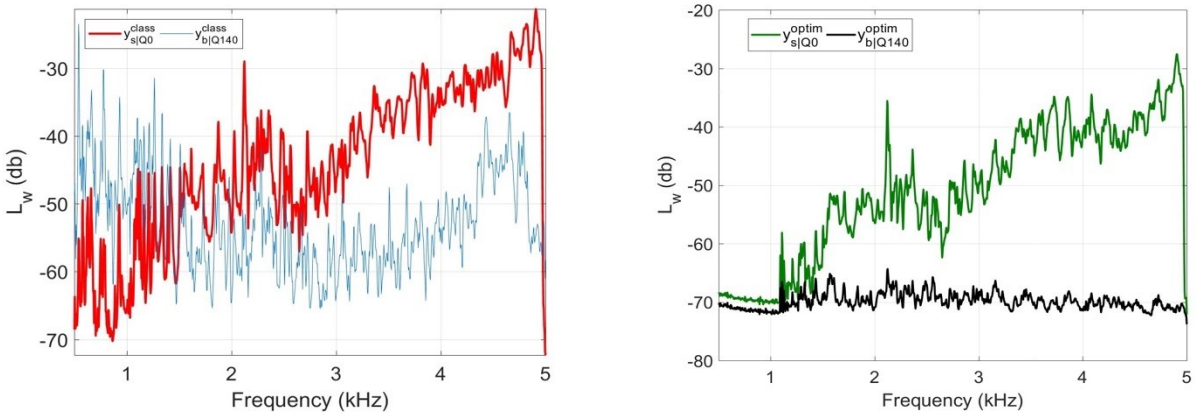


(a) (b)

Figure 7. Levels at the output of FV for the source only and for the noise only: (a), classical; (b), optimized.

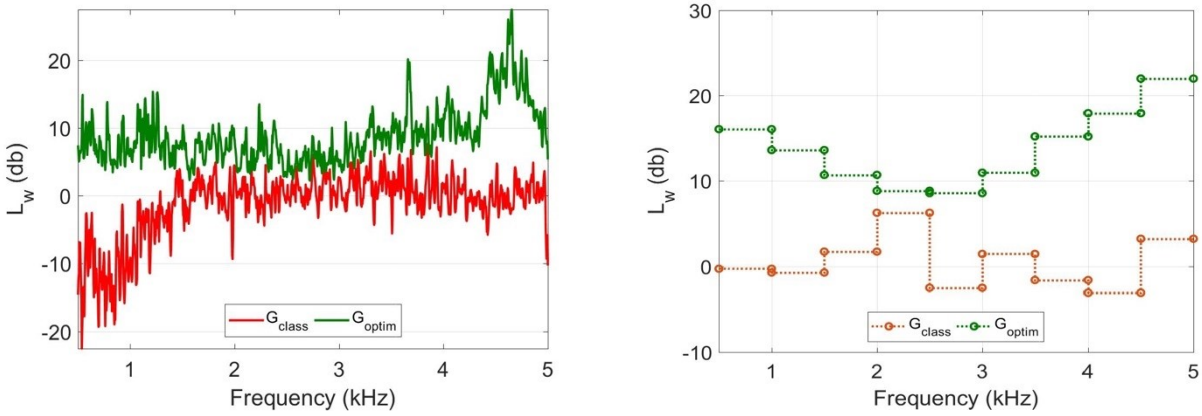


(a) (b)

Figure 8. (a) Gain comparison for classical and optimized beamfomring. (a) Narrow band beamforming ; (b) broadband beamforming.

## 6. Conclusions

The work presented in this paper occurred within a non-intrusive vibroacoustic technique study for the detection of a sodium-water reaction in a sodium-cooled nuclear reactor steam generator. The contribution of the vibroacoustic beamforming allows to detect the signal due to the source when it is embedded in a background noise. The study was conducted on a water test duct (a pipe) where the source to discriminate consists of a hydrophone in transmission mode placed inside the pipe while the disturbing noise is induced by the water turbulent flow. Instrumentation consisted of an array of 25 accelerometers placed on the duct.

Conventional beamforming appeared inoperative at high flow rates (i.e. typically $140\,\mathrm{l.s^{-1}}$) regardless of frequencies in the [500 Hz - 5 kHz] band. On the other hand, very significant effective gains over the entire frequency spectrum studied were observed using optimized beamforming. This is due to the definition of the steering vectors which takes into account the vibration noise spatial correlation. In broadband, gains ranging from 9 dB to 23 dB was obtained. It should nevertheless be noted that these gains results from considering "ideal" data to define the steering vectors:

- Source-sensor transfer functions considered were measured on the pipe.
- The cross-spectral matrix of accelerations characterizing the noise has been used both to define the steering vectors and to test the performance of the beamforming.

In the future, it will be necessary to develop a reliable vibroacoustic model of the test duct to predict source-sensor transfer functions because they are difficult to measure in practice. Moreover, a sensitivity study of the performance of the beamforming to the definition of the cross-spectral matrix of accelerations characterizing the noise is to be realized. Here it must be recalled that the majority of background noise in an operating steam generator is due to the combined noise of sodium flow and water evaporation, while we only assimilated it to turbulent flows.

## REFERENCES

[1] J. Moriot, L. Maxit, J. L. Guyader, O. Gastaldi, and J. Périsse, "Use of beamforming for detecting an acoustic source inside a cylindrical shell filled with a heavy fluid," *Mech. Syst. Signal Process.*, vol. 52–53, pp. 645–662, Feb. 2015.

[2] J. Moriot, "Détection vibro-acoustique passive d'une réaction sodium-eau par formation de voies dans un générateur de vapeur d'un réacteur nucléaire à neutrons rapides refroidi au sodium," Thèse de doctorat, INSA de Lyon, 2013.

[3] D. G. Manolakis, V. K. Ingle, and S. M. Kogon, *Statistical and adaptive signal processing*. Boston, London: ARTECH House, 2005.

[4] S. Loyka, "Maximum SNR Beamforming." ELG5132 Smart Antennas, 11-Oct-17.

[5] S. Kassab and L. Maxit, "Formation de voies vibroacoustique pour la détection d'une réaction sodium-eau: étude de l'impact des brides de fixation," in *Proceedings of CFA/ VISHNO 2016*, Le Mans, France, 2016.

[6] C. R. Fuller, "The effects of wall discontinuities on the propagation of flexural waves in cylindrical shells," *J. Sound Vib.*, vol. 75, no. 2, pp. 207–228, 1981.

[7] C. R. Fuller and F. J. Fahy, "Characteristics of wave propagation and energy distributions in cylindrical elastic shells filled with fluid," *J. Sound Vib.*, vol. 81, no. 4, pp. 501–518, 1982.

[8] S. Kassab, "Vibroacoustic beamforming for the detection of an acoustic monopole inside a thin cylindrical shell coupled to a heavy fluid: Numerical and experimental developments," Thèse de doctorat, Université de Lyon; INSA de Lyon, Lyon, 2018.